

# A study of nickel monoxide (NiO), nickel dioxide (ONiO), and Ni(O<sub>2</sub>) complex by anion photoelectron spectroscopy

Hongbin Wu and Lai-Sheng Wang

Department of Physics, Washington State University, Richland, Washington 99352 and Environmental Molecular Sciences Laboratory, Pacific Northwest National Laboratory, MS K2-14, P.O. Box 999, Richland, Washington 99352

(Received 13 February 1997; accepted 25 March 1997)

We report the first anion photoelectron spectroscopic study of nickel monoxide (NiO), nickel dioxide (ONiO), and nickel-O<sub>2</sub> complex, Ni(O<sub>2</sub>). The adiabatic electron affinity (EA) of NiO is measured to be 1.46 (2) eV. Five low-lying electronic excited states (*A*<sup>3</sup>Π, *a*<sup>1</sup>Δ, *B*<sup>3</sup>Φ, *b*<sup>1</sup>Σ<sup>+</sup>, *c*<sup>1</sup>Π) are observed for NiO at 0.43 (4), 0.94 (4), 1.24 (3), 1.80 (10), and 2.38 (10) eV above the ground state, respectively. Two isomers are observed for NiO<sub>2</sub>, i.e., the linear ONiO dioxide and the Ni(O<sub>2</sub>) complex. The dioxide has a high EA of 3.05 (1) eV while the Ni(O<sub>2</sub>) complex has a rather low EA of 0.82 (3) eV. Two low-lying excited states are observed for ONiO at 0.40 (2) and 0.77 (3) eV above the ground state, respectively. The vibrational frequency of the *v*<sub>1</sub> mode of the ground state ONiO (*X*<sup>3</sup>Σ<sub>g</sub><sup>-</sup>) is measured to be 750 (30) cm<sup>-1</sup>. The excited states of the Ni(O<sub>2</sub>) complex give broad photodetachment features starting at about 1.1 eV above the ground state. Information about the electronic structures of the nickel oxide species and chemical bonding between Ni and O and O<sub>2</sub> is obtained and discussed. © 1997 American Institute of Physics. [S0021-9606(97)00525-4]

## I. INTRODUCTION

Despite the importance of transition metal oxides in materials application and the oxidation of metal surfaces, our knowledge of simple transition metal oxide molecules is far from complete.<sup>1</sup> This is particularly true for nickel oxide. There have been several calculations<sup>2-5</sup> and experimental studies<sup>6-11</sup> about the nickel monoxide molecule (NiO), whose ground state is known to be a <sup>3</sup>Σ<sup>-</sup> state. But very little is known about its electronic excited states. The Ni(O<sub>2</sub>) complex has been studied both experimentally<sup>12,13</sup> and theoretically.<sup>14,15</sup> In the CuO<sub>2</sub> system, both a linear dioxide OCuO and a Cu(O<sub>2</sub>) complex are known to exist. However, it is not known if there exists a similar nickel dioxide molecule until very recently.<sup>13</sup>

As we have shown previously, photoelectron spectroscopy (PES) of anions with various detachment photon energies is particularly powerful to probe the low-lying electronic excited states of novel neutral species.<sup>16-26</sup> In spite of its intrinsic low-resolution nature, PES can provide unique electronic structure information which is otherwise difficult or impossible to obtain with other optical techniques. In the current work, we present the first PES study of NiO<sup>-</sup>, and ONiO<sup>-</sup>, and Ni(O<sub>2</sub>)<sup>-</sup>.

In addition to the electron affinities which are measured directly from the PES spectra, a wealth of electronic structure information is obtained about the corresponding neutral molecules. A total of five low-lying excited states are observed for NiO within 2.5 eV above its ground state. These states are assigned on the basis of its ground-state configuration and existing theoretical calculations. A very high EA is measured for the linear ONiO dioxide molecule. Besides the vibrationally resolved ground state, two excited states are observed for ONiO. The Ni(O<sub>2</sub>) complex is found to have a

rather low EA, consistent with a more weakly bound complex. The excited states of Ni(O<sub>2</sub>) exhibit broad spectral features.

In the following section, the experimental details are described. We present the PES results in Sec. III. Each molecule is discussed in detail in Sec. IV. Finally, a summary is given in Sec. V.

## II. EXPERIMENT

Our experimental apparatus has been described in detail before.<sup>26,27</sup> Briefly, it consists of a laser vaporization cluster source, a time-of-flight (TOF) mass spectrometer, and a magnetic-bottle TOF photoelectron analyzer. The NiO<sup>-</sup> anion is produced by vaporizing a pure nickel target with neat helium carrier gas, due to the surface oxide layer on the target (Fig. 1). When helium carrier gas seeded with 0.1% O<sub>2</sub> is used, abundant NiO<sub>2</sub><sup>-</sup> is produced with little NiO<sup>-</sup> formed. Two types of cluster nozzles are used to produce the NiO<sub>2</sub><sup>-</sup> species, one with a large waiting room, as described before,<sup>27</sup> and one without the large waiting room. We find that the large waiting room nozzle produces both the Ni(O<sub>2</sub>)<sup>-</sup> complex and the ONiO<sup>-</sup> dioxide (Fig. 2) while the nozzle without the large waiting room produces exclusively the ONiO<sup>-</sup> dioxide (Fig. 3). The Ni(O<sub>2</sub>)<sup>-</sup> complex, similar to our previously observed Cu(O<sub>2</sub>)<sup>-</sup> complex,<sup>16</sup> is likely formed during the supersonic expansion from the 2 mm diam throat of the large waiting room nozzle.<sup>27</sup> The condition that optimizes the formation of the Ni(O<sub>2</sub>)<sup>-</sup> complex is at the leading edge of the carrier gas pulse, where more abundant Ni<sup>-</sup> atomic species is found. This condition is unfavorable for the cooling of the ONiO<sup>-</sup> species (the optimal cooling is at the peak of the carrier gas pulse), clearly shown by the hot bands observed for the spectrum of ONiO<sup>-</sup> in Fig. 2.

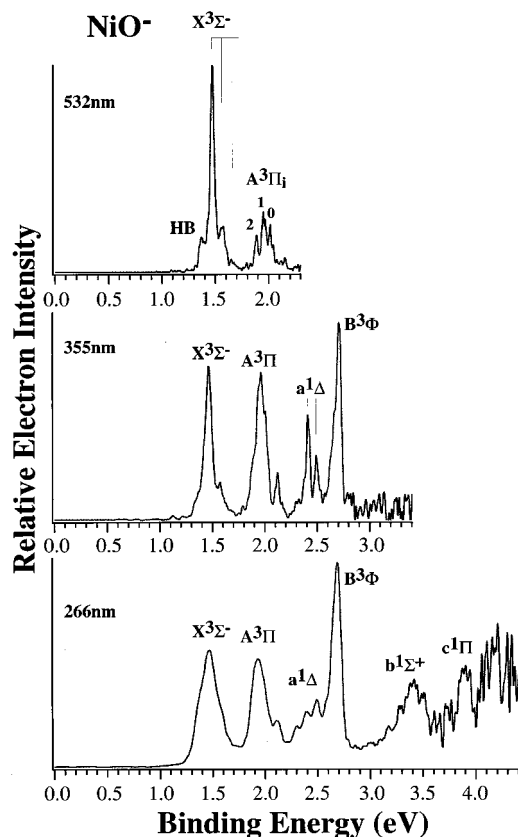


FIG. 1. Photoelectron spectra of  $\text{NiO}^-$  at 532 nm (2.33 eV), 355 nm (3.49 eV), and 266 nm (4.66 eV). The spectral assignments and vibrational structures are indicated. HB stands for hot bands.

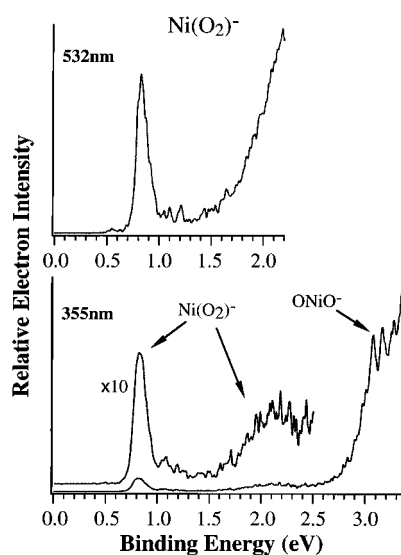


FIG. 2. Photoelectron spectra of  $\text{Ni}(\text{O}_2)^-$  complex at 532 and 355 nm. The 355 nm spectrum also contains spectral features from the  $\text{ONiO}^-$  dioxide molecule (see Fig. 3 and the text). Weak features around 1.2 eV are due to  $\text{Ni}^-$  as a result of photodissociation of the parent  $\text{Ni}(\text{O}_2)^-$  anion.

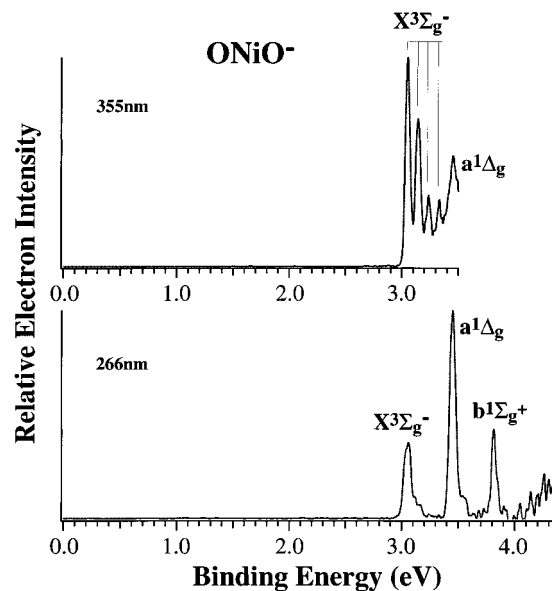


FIG. 3. Photoelectron spectra of  $\text{ONiO}^-$  dioxide at 355 and 266 nm. Note the high electron affinity of the  $\text{ONiO}^-$  molecule and the well resolved vibrational progression in the 355 nm spectrum.

The negative ions from the collimated supersonic beam are extracted at  $90^\circ$  into the TOF mass spectrometer. The cluster of interest is selected and decelerated before detached by a laser beam from a Q-Switched Nd:YAG laser (532, 355, and 266 nm). Nearly 100% of the emitted electrons are collected by the magnetic bottle and analyzed by a 3.5 m long TOF tube. The measured electron TOF spectra are calibrated using the known spectrum of  $\text{Cu}^-$ .<sup>25</sup> The presented electron binding energy spectra are obtained by subtracting the calibrated kinetic energy spectra from the respective photon energies used for detachment. Low photon energies are used to obtain better resolved spectra due to the energy dependence of the energy resolution in the TOF-type electron analyzer. Higher photon energies are used to obtain more highly excited states of the neutral species. The resolution of the current spectrometer is better than 30 meV at 1 eV electron energy.<sup>25</sup>

### III. RESULTS

Figure 1 shows the photoelectron spectra of  $\text{NiO}^-$  at three photon energies. The 532 nm spectrum reveals two electronic states of the NiO molecule with partially resolved vibrational structures. Two more states at 2.4 and 2.7 eV binding energies (BEs) are further revealed at 355 nm. The 2.4 eV state shows a vibrational progression while the 2.7 eV peak is sharp and intense. More states are revealed at 266 nm, but the signal-to-noise ratio is rather poor at the high BE side. Nevertheless, at least two states can be identified at about 3.3 and 3.8 eV. The BEs of all these states and the obtained spectroscopic constants are listed in Table I.

Figure 2 shows the spectra of  $\text{Ni}(\text{O}_2)^-$  at 532 and 355 nm when the large waiting room nozzle is used to produce the  $\text{Ni}(\text{O}_2)^-$  species. The 532 nm spectrum shows a sharp feature at 0.82 eV and the onset of a broad band following an energy

TABLE I. Observed binding energies (BE) and spectroscopic constants for NiO<sup>-</sup> and NiO.

	State	BE (eV)	Term value (eV)		Vib. freq. (cm <sup>-1</sup> )	
			This work	Previous	This work	Previous
NiO <sup>-</sup>	X( <sup>2</sup> Π)				810(50)	
NiO	X( <sup>3</sup> Σ <sup>-</sup> )	1.46(2) <sup>a</sup>	0		800(50)	839 <sup>d</sup>
	A( <sup>3</sup> Π <sub>2</sub> )	1.89(4)	0.43(4)			
	( <sup>3</sup> Π <sub>1</sub> )	1.95(5)	0.49(5)			
	( <sup>3</sup> Π <sub>0</sub> )	2.01(6)	0.55(6)	0.537 <sup>b</sup>		780.8 <sup>b</sup>
				0.532 <sup>c</sup>		777.1 <sup>c</sup>
	a( <sup>1</sup> Δ)	2.41(4)	0.94(4)		680(60)	
	B( <sup>3</sup> Φ)	2.70(2)	1.24(3)			
	b( <sup>1</sup> Σ <sup>+</sup> )	3.26(10)	1.80(10)			
	c( <sup>1</sup> Π)	3.84(10)	2.38(10)			

<sup>a</sup>Adiabatic electron affinity of NiO.<sup>b</sup>From Ref. 10.<sup>c</sup>From Ref. 9.<sup>d</sup>From Ref. 8.

gap. There are weak features around 1.2 eV which can be attributed to detachment features of Ni<sup>-</sup>. This suggests that there is a weak dissociation channel, NiO<sub>2</sub><sup>-</sup> → Ni<sup>-</sup> + O<sub>2</sub>. Similar dissociation processes have been observed for the Cu(O<sub>2</sub>)<sup>-</sup> complex previously,<sup>16,25</sup> suggesting that we are dealing with a Ni(O<sub>2</sub>)<sup>-</sup> complex currently. The 355 nm spectrum shows a broad band at about 2 eV, in addition to the sharp peak at 0.82 eV. However, much stronger features are revealed near 3 eV [Note the × 10 amplification for the features due to the Ni(O<sub>2</sub>)<sup>-</sup> complex.]

Figure 3 shows the spectra of NiO<sub>2</sub><sup>-</sup> at 355 and 266 nm when the nozzle without the large waiting room is used. The 355 nm spectrum is drastically different from the one shown in Fig. 2. The weak features at lower BE disappear and the strong features near 3 eV become a nice vibrational progression. A peak near 3.45 eV is also observed, which becomes an intense and sharp feature in the 266 nm spectrum (Fig. 3, lower panel). In addition, the 266 nm spectrum reveals one extra sharp feature near 3.82 eV, with indications of even higher BE features. Therefore, it is clear that we are dealing with two isomers of NiO<sub>2</sub><sup>-</sup>. The first isomer (Fig. 2) is a NiO<sub>2</sub> complex; on the basis of the high EA of the second isomer (Fig. 3), we assign it to be a yet known ONiO<sup>-</sup> dioxide. These two isomers are analogous to the two isomers that exist for the CuO<sub>2</sub> system.<sup>16</sup> The 355 nm spectrum of Fig. 2 clearly contains features from both isomers while Fig. 3 shows the features only from the ONiO<sup>-</sup> isomer. The different populations of the two isomers are due to the two different nozzles used, as described above. It is also worth noting that the vibrational progression observed in the 355 nm spectrum of ONiO<sup>-</sup> seems to disappear in the 266 nm spectrum (Fig. 3). The BEs and the obtained spectroscopic constants are listed in Table II for both the Ni(O<sub>2</sub>) complex and the ONiO dioxide. In the following, we discuss each molecule individually.

## IV. DISCUSSION

### A. NiO

Several calculations have been performed on the electronic structure of the NiO diatomic and its ground-state

properties are well understood.<sup>2-11</sup> The bonding between Ni and O can be viewed as Ni<sup>+</sup>O<sup>-</sup> with substantial covalent character. The valence molecular orbitals (MOs) of NiO can be considered as derived from Ni<sup>+</sup> and O<sup>-</sup>, as schematically shown in Fig. 4. The <sup>3</sup>Σ<sup>-</sup> ground state of NiO is well established with the 1σ<sup>2</sup>1π<sup>4</sup>1δ<sup>4</sup>2σ<sup>2</sup>2π<sup>2</sup> configuration. The 1σ and 1π MOs are bonding orbitals between O2pσ-3dσ and O2pπ-3dπ, respectively; the 2σ and 2π MOs are slightly antibonding; the 1δ is a nonbonding MO with pure 3d character. In the NiO<sup>-</sup> anion, the extra electron is expected to enter the 2π orbital to give a 1σ<sup>2</sup>1π<sup>4</sup>1δ<sup>4</sup>2σ<sup>2</sup>2π<sup>3</sup> configuration, with a <sup>2</sup>Π ground state. As pointed out in the recent theoretical work,<sup>5</sup> the three MOs, 1δ, 2σ, and 2π, are relatively close in energy and are well separated from the 1σ and 1π bonding MOs. Therefore, it is possible that the photodetachment can take place from all these three MOs at the current photon energies. The configurations and electronic states resulting from these detachment processes are as follows:

- (1) 1σ<sup>2</sup>1π<sup>4</sup>1δ<sup>4</sup>2σ<sup>2</sup>2π<sup>3</sup>(<sup>2</sup>Π) → 1σ<sup>2</sup>1π<sup>4</sup>1δ<sup>4</sup>2σ<sup>2</sup>2π<sup>2</sup>:  
<sup>3</sup>Σ<sup>-</sup>, <sup>1</sup>Δ, <sup>1</sup>Σ<sup>+</sup>;
- (2) 1σ<sup>2</sup>1π<sup>4</sup>1δ<sup>4</sup>2σ<sup>2</sup>2π<sup>3</sup>(<sup>2</sup>Π) → 1σ<sup>2</sup>1π<sup>4</sup>1δ<sup>4</sup>2σ<sup>1</sup>2π<sup>3</sup>:  
<sup>3</sup>Π, <sup>1</sup>Π;
- (3) 1σ<sup>2</sup>1π<sup>4</sup>1δ<sup>4</sup>2σ<sup>2</sup>2π<sup>3</sup>(<sup>2</sup>Π) → 1σ<sup>2</sup>1π<sup>4</sup>1δ<sup>3</sup>2σ<sup>2</sup>2π<sup>3</sup>:  
<sup>3</sup>Φ, <sup>3</sup>Π, <sup>1</sup>Φ, <sup>1</sup>Π.

TABLE II. Observed binding energies (BE) and spectroscopic constants for Ni(O<sub>2</sub>) and ONiO.

	State	BE (eV)	Term value (eV)	Vib. freq. (cm <sup>-1</sup> )
Ni(O <sub>2</sub> )	X	0.82(3) <sup>a</sup>	0	
	A	~1.8	~1	
ONiO	X( <sup>3</sup> Σg <sup>-1</sup> )	3.05(1) <sup>b</sup>	0	750(30)
	a( <sup>1</sup> Δg)	3.45(2)	0.40(2)	
	b( <sup>1</sup> Σg <sup>+</sup> )	3.82(3)	0.77(3)	

<sup>a</sup>Adiabatic electron affinity of Ni(O<sub>2</sub>).<sup>b</sup>Adiabatic electron affinity of ONiO.

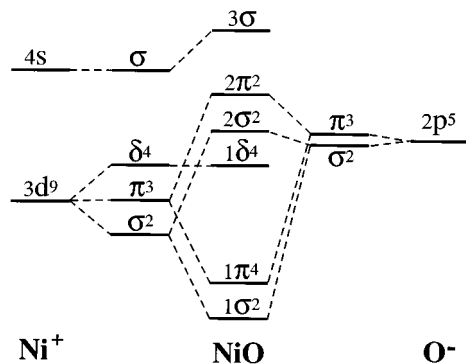


FIG. 4. A schematic molecular orbital diagram for the NiO molecule.

All of these states can be accessed in the photodetachment transitions, depending on their excitation energies relative to the ground state. However, besides the ground state ( $X^3\Sigma^-$ ), only five excited states are observed. Our assignments are indicated in Fig. 1 and the obtained spectroscopic constants are given in Table I.

The vibrational frequency obtained for the ground state ( $X^3\Sigma^-$ ) is  $800 (50) \text{ cm}^{-1}$  which agrees with the previous optical measurements (Table I). The first excited state at a BE of 1.89 eV appears to consist of a vibrational progression. However, the separation among the three features is about  $60 \text{ meV} (480 \text{ cm}^{-1})$ , which seems to be too small compared to that of the ground state. Previous optical experiments have identified a  $^3\Pi_i$  excited state at about 0.53 eV above the ground state for the transition between the  $^3\Sigma^-$  ground state and the  $^3\Pi_0$  spin-orbit state.<sup>9,10</sup> This excitation energy is in excellent agreement with that corresponding to the third feature at a BE of 2.01 eV (Table I). Thus this peak is assigned to the  $^3\Pi_0$  component of the  $^3\Pi$  state resulting from (2) by removing a  $2\sigma$  electron. Since the MO configuration corresponding to the  $^3\Pi$  state is more than half-filled, the spin-orbit components have the following order,  $^3\Pi_2$ ,  $^3\Pi_1$ ,  $^3\Pi_0$ , with increasing energy. Therefore, the peak at 1.89 eV BE is assigned to the  $^3\Pi_2$  spin-orbit state, which was not observed in the previous optical experiments. The second peak at a BE of 1.95 eV is then assigned to the  $^3\Pi_1$  spin-orbit state, as shown in Fig. 1.

However, this assignment yields a spin-orbit splitting (about  $480 \text{ cm}^{-1}$ ) which is much larger than that measured in the previous optical experiments ( $283.37 \text{ cm}^{-1}$  from Ref. 10 and  $349.21 \text{ cm}^{-1}$  from Ref. 9 between the  $\Omega = 0$  and 1 components). The currently obtained spin-orbit splitting is reasonable compared to that found in Ni atom,<sup>28</sup> and clearly more accurate calculations or much higher resolution PES spectrum of  $\text{NiO}^-$  will be required to resolve this issue. In any case, there is no doubt that the first excited state of the NiO molecule is the  $A^3\Pi$  state from (2). Each spin-orbit state is expected to have its own vibrational progression, which may overlap with states from the higher spin-orbit states. This overlap probably complicates the PES spectrum in Fig. 1. The feature near a BE of 2.12 eV, which is shown more clearly in the 355 and 266 nm spectra, is likely due to the  $v = 1$  vibrational state of the  $^3\Pi_0$  spin-orbit state.

The second excited state at a BE of 2.41 eV has a nice vibrational progression with a vibrational frequency of  $680 (60) \text{ cm}^{-1}$  and a 0.94 eV excitation energy from the ground state. This state is assigned to the  $^1\Delta$  state. The sharp and simple vibrational progression observed suggests that there is no spin-orbit splitting complication, consistent with the assignment.

The state with a BE of 2.70 eV is sharp and intense with an excitation energy of 1.24 eV above the ground state. It shows no vibrational progression, suggesting that the detached electron is from a nonbonding orbital. It is natural to assign this state to the  $^3\Phi$  state, due to the detachment of a nonbonding  $\delta$  electron as shown in (3) above. The width of the observed peak is about  $75 \text{ meV}$  (FWHM), much broader than the experimental resolution at this energy, indicating that this peak probably contains spin-orbit components, consistent with the assignment to the  $^3\Phi$  state.

The higher excited states observed at the 266 nm in Fig. 1 are less well defined due to the poor signal-to-noise ratio. The state at a BE of 3.26 eV shows a vibrational progression and gives an excitation energy of about 1.8 eV. This state is tentatively assigned to the  $^1\Sigma^+$  state of (1) above. Another state at a BE of 3.84 eV is tentatively assigned to the  $^1\Pi$  state of (2), arising from the same configuration as that of the  $A^3\Pi$  state. The three higher energy states arising from detachment of a  $1\delta$  electron ( $^3\Pi$ ,  $^1\Phi$ , and  $^1\Pi$ ) are expected to give sharp features similar to the  $^3\Phi$  state and probably have PES binding energies above 4 eV.

The  $A^3\Pi$  state is the only previously characterized excited state for the NiO molecule experimentally. Theoretically, Bauschlicher *et al.* has calculated an excitation energy for the  $^3\Pi$  state at 0.518 eV ( $4180 \text{ cm}^{-1}$ ) which agrees well with the experiments.<sup>3</sup> However, the same level of theory gives an excitation energy for the  $^3\Phi$  state at 0.853 eV ( $6880 \text{ cm}^{-1}$ ), which is apparently too small compared to the current experiment. Walch and Goddard have calculated 20 low-lying excited states for NiO, but the ordering of the states disagrees with the experiments.<sup>2</sup> In particular, the first excited state was calculated to be the  $^1\Delta$  state. The current experiments provide a rather complete set of energy levels for the low-lying excited states of NiO within 2.5 eV of the ground state and will be valuable to compare with more accurate calculations that intends to correctly treat simple molecules containing a Ni atom.

## B. $\text{Ni}(\text{O}_2)$ complex

The  $\text{Ni}(\text{O}_2)$  complex has a symmetric side-on  $C_{2v}$  structure, as concluded from two previous theoretical calculations and two low temperature matrix experiments.<sup>12-15</sup> The calculations indicated that the  $\text{Ni}(\text{O}_2)$  complex has a singlet  $^1A_1$  ground state.<sup>14,15</sup> The interaction between Ni and  $\text{O}_2$  involves both ionic and covalent bonding: The ionic character comes from the transfer of the Ni 4s electrons to the out of plane  $\pi_g$  orbital on  $\text{O}_2$  and the covalent bonding is between the Ni 3d and the in-plane  $\pi_g$  orbital. The HOMO and

LUMO of Ni(O<sub>2</sub>) derive from the bonding and antibonding interactions between the 3*d<sub>xz</sub>* and the π<sub>g</sub> orbitals, respectively.

The PES spectra of Ni(O<sub>2</sub>) (Fig. 2) show a sharp threshold peak at 0.82 eV and a broad feature starting at about 1.8 eV with a large energy gap (about 1 eV). The sharp feature yields the EA for Ni(O<sub>2</sub>) to be 0.82 (3) eV, which is smaller than the EA of both Ni (1.156 eV)<sup>29</sup> and NiO (Table I), but higher than that of O<sub>2</sub> (0.451 eV).<sup>30</sup> The low EA for Ni(O<sub>2</sub>) suggests that it is a weakly-bonded complex and that the extra electron in the Ni(O<sub>2</sub>)<sup>-</sup> anion is shared between Ni and O<sub>2</sub>. This is consistent with the character of the Ni(O<sub>2</sub>) LUMO, which is derived from the combination of the Ni 4*s* and O<sub>2</sub> π<sub>g</sub> orbitals. The narrow peak width of the threshold feature is in sharp contrast to the broad Franck–Condon envelope observed for the detachment of O<sub>2</sub><sup>-</sup>.<sup>30</sup> This implies that the extra electron in Ni(O<sub>2</sub>)<sup>-</sup> is probably more localized on the Ni atom, understandably due to the high EA of the Ni atom. The observed energy gap in the PES spectra is also consistent with the theoretical calculations that the Ni(O<sub>2</sub>) complex is a closed shell, singlet molecule (*X*<sup>1</sup>A<sub>1</sub>).

In the spectra shown in Fig. 2, very weak signals due to Ni<sup>-</sup> at around 1.2 eV can be seen, arising from a two-photon process: Ni(O<sub>2</sub>)<sup>-</sup> → Ni<sup>-</sup> + O<sub>2</sub> and subsequent detachment of the Ni<sup>-</sup> product within the same laser pulse (7 ns pulse width). In the Cu(O<sub>2</sub>)<sup>-</sup> case reported previously,<sup>17</sup> we observed a much higher level of dissociation: Cu(O<sub>2</sub>)<sup>-</sup> → Cu<sup>-</sup> + O<sub>2</sub>. This implies that the bonding between Ni–O<sub>2</sub> is stronger than that in Cu(O<sub>2</sub>), in agreement with previous works.<sup>14,15</sup>

The detachment transition to the excited states of Ni(O<sub>2</sub>) (Fig. 2) displays a broad feature starting at about 1.8 eV, i.e., about 1 eV above the ground state, indicating a large geometry change from the ground state of the anion. As suggested from the previous theoretical works,<sup>14,15</sup> the O–O bond is significantly stretched in Ni(O<sub>2</sub>). We suspect that there might be an O–O bond rupture in the excited state of Ni(O<sub>2</sub>) to form the ONiO molecule, suggesting the reaction barrier between Ni + O<sub>2</sub> is less than 1 eV. Alternatively, there might be a predissociation in the excited state of Ni(O<sub>2</sub>). This would suggest the Ni–O<sub>2</sub> bond energy to be less than 1 eV (23 kcal/mol). The latter suggestion is consistent with the calculation by Blomberg *et al.* who obtained a bond energy of 18 kcal/mol,<sup>14</sup> but disagrees with the calculation by Bauschlicher *et al.* who obtained a bond energy of 48 (7) kcal/mol.<sup>15</sup> In any case, further theoretical calculations are warranted in light of the current experiment which provides both the EA of Ni(O<sub>2</sub>) and information about the nature and position of its excited states.

### C. Nickel dioxide, ONiO

The only calculation for the ONiO dioxide was done by Blomberg *et al.* who considered the O<sub>2</sub> chemisorption on Ni surfaces and used Ni + O<sub>2</sub> as the simplest case.<sup>14</sup> The room temperature reaction between Ni and O<sub>2</sub> leads to the Ni(O<sub>2</sub>) complex and the ONiO dioxide has never been observed in the gas phase. The formation of the ONiO<sup>-</sup> mol-

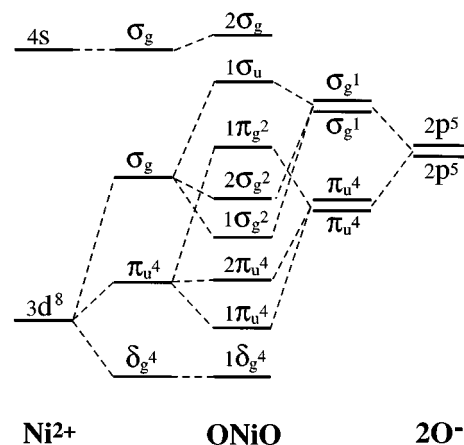


FIG. 5. A schematic molecular orbital diagram for the linear ONiO dioxide molecule.

ecule in our laser vaporization experiment is due to the high-energy conditions of the laser-induced plasma. The ONiO molecule has recently been observed in low-temperature matrix experiment, also produced from a laser vaporization source.<sup>13</sup> The PES spectra in Fig. 3 yield a very high EA of 3.05 eV for the ONiO molecule, much higher than that of the NiO molecule (Table I). This is consistent with a dioxide molecule, suggesting that the oxidation state of Ni is increased, compared to the monoxide. We have found previously that the EAs of metal oxide clusters generally increase with the number of O atoms in the clusters up to the maximum oxidation states of the metal element.<sup>21–25</sup>

The 355 nm PES spectrum of ONiO<sup>-</sup> (Fig. 3) shows a simple and well resolved vibrational progression with a frequency of 750 cm<sup>-1</sup>, as well as the onset of an excited-state feature at 3.45 eV. This feature becomes a sharp and intense peak in the 266 nm spectrum. In addition, the 266 nm spectrum shows another sharp excited-state feature at 3.82 eV. There is also evidence for more excited states beyond 4 eV. It is surprising that the nice vibrational progression observed in the 355 nm spectrum seems to disappear in the 266 nm spectrum, which shows significantly reduced intensities for the higher vibrational levels of the ONiO ground state. This photon energy-dependence suggests that there is an autodetachment process that enhances the Franck–Condon factors for the higher vibrational levels at the 355 nm detachment photon energy.

The bonding of the ONiO dioxide is expected to be similar to the linear OCuO molecule. It is likely that the ONiO molecule is also linear. A similar conclusion has been arrived from the recent matrix experiment, that yields an anti-symmetric vibrational frequency ( $\nu_3$ ) of 945.4 cm<sup>-1</sup> for the linear ONiO molecule.<sup>13</sup> Our measured frequency of 750 cm<sup>-1</sup> for the ground state of ONiO should correspond to the symmetric vibrational mode ( $\nu_1$ ).

In analogy with OCuO, the bonding in ONiO may be viewed as O<sup>-</sup>Ni<sup>2+</sup>O<sup>-</sup> including both ionic and covalent interactions. Figure 5 shows a schematic MO diagram adapted from that for OCuO.<sup>16</sup> The OCuO molecule has a single 1 π<sub>g</sub> hole (π<sub>g</sub><sup>3</sup>) with a <sup>2</sup>Π<sub>g</sub> ground state, while the OCuO<sup>-</sup>

anion has a closed shell configuration with a singlet ground state  $^1\Sigma_g^+$ . The Ni atom has one less valence electron than the Cu atom and the ONiO molecule is expected to have two  $1\pi_g$  holes ( $\pi_g^2$ ), with a  $^3\Sigma_g^-$  ground state. The ONiO<sup>-</sup> anion then is expected to have a  $1\pi_g^3$  configuration similar to the OCuO neutral ground state. Detachment of one  $1\pi_g$  electron will result in two excited state ( $^1\Delta_g$  and  $^1\Sigma_g^-$ ), along with the  $^3\Sigma_g^-$  ground state. The observed PES features are assigned to these three states as shown in Fig. 3. The three observed states show similar sharp spectral features and no spin-orbit splitting is apparent (the latter would broaden and complicate the spectral features as seen above in the NiO case). These observations are consistent with the assignments. Finally, it is interesting to note that the splitting among the three states ( $^3\Sigma_g^-$ ,  $^1\Delta_g$ ,  $^1\Sigma_g^+$ ) resulting from the  $2\pi^2$  ground-state configuration of NiO is much larger than that among the three states resulting from the  $1\pi_g^2$  ground-state configuration of the linear ONiO. This is likely due to the fact that the  $1\pi_g$  orbital of ONiO, with considerable  $O2p$  character, is delocalized over a much larger space than that of the  $2\pi$  orbital of NiO. This is expected and further supports the assignments for these electronic states of ONiO.

## V. CONCLUSIONS

In summary, the first photoelectron spectra of the nickel monoxide (NiO), Ni(O<sub>2</sub>) complex, and the linear ONiO di-oxide are reported and information about their electronic structures and chemical bonding are obtained and discussed. Electron affinities, vibrational frequencies, and excited state energy levels are presented. The current work provides direct experimental electronic structure information and spectroscopic parameters that can be used to benchmark further theoretical calculations. Considering the importance of the Ni-oxygen chemical interactions, further high level calculations on these systems are indeed called for.

## ACKNOWLEDGMENTS

Support for this research from the National Science Foundation under Grant No. CHE-9404428 is gratefully acknowledged. The work is performed at Pacific Northwest

National Laboratory, operated for the U.S. Department of Energy by Battelle under Contract No. DE-AC06-76RLO 1830.

- <sup>1</sup>(a) A. J. Merer, *Annu. Rev. Phys. Chem.* **40**, 407 (1989); (b) K. P. Huber and G. Herzberg, *Molecular Spectra and Molecular Structure. IV. Constants of Diatomic Molecules* (Van Nostrand Reinhold, New York, 1979).
- <sup>2</sup>S. P. Walch and W. A. Goddard III, *J. Am. Chem. Soc.* **100**, 1338 (1978).
- <sup>3</sup>C. W. Bauschlicher, Jr., *Chem. Phys.* **93**, 399 (1985); C. W. Bauschlicher, Jr., C. J. Nelin, and P. S. Bagus, *J. Chem. Phys.* **82**, 3265 (1985); C. W. Bauschlicher, Jr. and P. Maitre, *Theor. Chim. Acta* **90**, 189 (1995).
- <sup>4</sup>M. Dolg, U. Wedig, H. Stoll, and H. Preuss, *J. Chem. Phys.* **86**, 2123 (1987).
- <sup>5</sup>E. G. Bakalbassis, M. D. Stiakaki, A. C. Tsipis, and C. A. Tsipis, *Chem. Phys.* **205**, 389 (1996).
- <sup>6</sup>B. Rosen, *Nature (London)* **156**, 570 (1945).
- <sup>7</sup>D. W. Green and G. T. Reedy, *J. Mol. Spectrosc.* **78**, 257 (1979).
- <sup>8</sup>V. I. Srdanov and D. O. Harris, *J. Chem. Phys.* **89**, 2748 (1988).
- <sup>9</sup>E. J. Friedman-Hall and R. W. Field, *J. Mol. Spectrosc.* **155**, 259 (1992).
- <sup>10</sup>R. S. Ram and P. F. Bernath, *J. Mol. Spectrosc.* **155**, 315 (1992).
- <sup>11</sup>K. Namiki and S. Saito, *Chem. Phys. Lett.* **252**, 343 (1996).
- <sup>12</sup>H. Huber, W. Klotzbucher, G. A. Ozin, and A. V. Voet, *Can. J. Chem.* **51**, 2722 (1973).
- <sup>13</sup>A. Citra, G. V. Chertihin, L. Andrews, and M. Neurock (unpublished).
- <sup>14</sup>M. R. A. Blomberg, P. E. M. Siegbahn, and A. Strich, *Chem. Phys.* **97**, 287 (1985).
- <sup>15</sup>C. W. Bauschlicher, S. R. Langhoff, H. Partridge, and M. Sodupe, *J. Phys. Chem.* **97**, 856 (1993).
- <sup>16</sup>H. Wu, S. R. Desai, and L. S. Wang, *J. Chem. Phys.* **103**, 4363 (1995).
- <sup>17</sup>J. Fan and L. S. Wang, *J. Phys. Chem.* **98**, 11814 (1994); J. Fan, L. Lou, and L. S. Wang, *ibid.* **102**, 2701 (1995); L. S. Wang, *Surf. Rev. Lett.* **3**, 423 (1996).
- <sup>18</sup>J. Fan and L. S. Wang, *J. Chem. Phys.* **102**, 8714 (1995).
- <sup>19</sup>H. Wu, S. R. Desai, and L. S. Wang, *Phys. Rev. Lett.* **76**, 212 (1996).
- <sup>20</sup>L. S. Wang, H. Wu, S. R. Desai, J. Fan, and S. D. Colson, *J. Phys. Chem.* **100**, 8697 (1996).
- <sup>21</sup>L. S. Wang, H. Wu, S. R. Desai, and L. Lou, *Phys. Rev. B* **53**, 8028 (1996).
- <sup>22</sup>H. Wu, S. R. Desai, and L. S. Wang, *J. Am. Chem. Soc.* **118**, 5296 (1996).
- <sup>23</sup>L. S. Wang, H. Wu and S. R. Desai, *Phys. Rev. Lett.* **76**, 4853 (1996).
- <sup>24</sup>S. R. Desai, H. Wu, C. Rohlfing, and L. S. Wang, *J. Chem. Phys.* **106**, 1309 (1997).
- <sup>25</sup>H. Wu, S. R. Desai, and L. S. Wang, *J. Phys. Chem.* **101**, 2103 (1997).
- <sup>26</sup>H. Wu, S. R. Desai, and L. S. Wang, *Phys. Rev. Lett.* **77**, 2436 (1996).
- <sup>27</sup>L. S. Wang, H. S. Cheng, and J. Fan, *J. Chem. Phys.* **102**, 9480 (1995).
- <sup>28</sup>C. E. Moore, *Atomic Energy Levels*, Natl. Bur. Stand. Circ. (U.S. GPO, Washington D.C. 1971), Vol. II.
- <sup>29</sup>H. Hotop and W. C. Lineberger, *J. Phys. Chem. Ref. Data* **14**, 731 (1985).
- <sup>30</sup>R. J. Celotta, R. A. Bennett, J. L. Hall, M. W. Siegel, and J. Levine, *Phys. Rev. A* **6**, 631 (1972); L. A. Posey, M. J. Deluca, and M. A. Johnson, *Chem. Phys. Lett.* **131**, 170 (1986).